A Posteriori Error Estimates for Higher Order Godunov Finite Volume Methods on Unstructured Meshes

Timothy J. Barth and Mats G. Larson
NASA Technical Report NAS-02-001
February 2002
(Also appears in the Proceedings of FVCA, Porquerolles, France, June 2002.)

A posteriori error estimates for high order Godunov finite volume methods are presented which exploit the two solution representations inherent in the method, viz. as piecewise constants u_0 and cellwise p-th order reconstructed functions $R_p^0 u_0$. Using standard duality arguments, we construct exact error representation formulas for derived functionals that are tailored to the class of high order Godunov finite volume methods with data reconstruction, $R_p^0 u_0$. We then devise computable error estimates that exploit the structure of Godunov finite volume methods. The present theory applies directly to a wide range of finite volume methods in current use including MUSCL, TVD, UNO, and ENO methods. Issues such as the treatment of nonlinearity and post-processing of dual (adjoint) problem data are discussed. Numerical results for linear advection and nonlinear scalar conservation laws at steady-state are presented to validate the analysis.

A Posteriori Error Estimates for Higher Order Godunov Finite Volume Methods on Unstructured Meshes

Timothy J. Barth*[1] — Mats G. Larson**

**NASA Ames Research Center,*
Information Sciences Directorate,
Moffett Field, California, USA.
barth@nas.nasa.gov

***Chalmers Institute for Technology,*
Department of Mathematics,
Finite Element Center,
Göteborg, Sweden.
mgl@math.chalmers.se

ABSTRACT. *A posteriori error estimates for high order Godunov finite volume methods are presented which exploit the two solution representations inherent in the method, viz. as piecewise constants u_0 and cellwise p-th order reconstructed functions $R_p^0 u_0$. Using standard duality arguments, we construct exact error representation formulas for derived functionals that are tailored to the class of high order Godunov finite volume methods with data reconstruction, $R_p^0 u_0$. We then devise computable error estimates that exploit the structure of Godunov finite volume methods. The present theory applies directly to a wide range of finite volume methods in current use including MUSCL, TVD, UNO, and ENO methods [LEE 79, HAR 83, HAR 87, HAR 89, SHU 88, BAR 89, BAR 90, DUR 90, BAR 98, ABG 94, VAN 93]. Issues such as the treatment of nonlinearity and post-processing of dual (adjoint) problem data are discussed. Numerical results for linear advection and nonlinear scalar conservation laws at steady-state are presented to validate the analysis.*

KEYWORDS: *A posteriori error estimates, Godunov finite volume methods, discontinuous Galerkin methods, unstructured meshes.*

1. Corresponding author. No copyright is asserted in the United States under Title 17, U.S. Code. All other rights are reserved by the copyright owner.

1. Introduction

A frequent objective in numerically solving partial differential equations is the subsequent calculation of certain derived quantities of particular interest, e.g., aerodynamic lift and drag coefficients, stress intensity factors, mean temperatures, etc. Consequently, there is considerable interest in constructing *a posteriori* error estimates for such derived quantities (mathematically described as functionals) so as to improve the reliability and efficiency of numerical computations. For an introduction to *a posteriori* error analysis see the articles by Becker and Rannacher [BEC 98], Eriksson et al. [ERI 95], Giles et al. [GIL 97, GIL 99], Johnson et al. [JOH 95], Parashivoiu et al. [PER 97], Prudhomme and Oden [ODE 99, PRU 99], Süli [Sul 98], and the collected NATO lecture notes [BAR 02].

This article revisits the topic of *a posteriori* error estimation of user prescribed functionals with specific consideration given to finite volume methods that are extensions of Godunov's original method [GOD 59] to high order accuracy via various forms of data reconstruction, e.g. MUSCL in [LEE 79], TVD in [HAR 83], UNO in [HAR 87], ENO in [HAR 89, SHU 88] with faithful generalizations of Godunov's method to unstructured meshes given in [BAR 89, BAR 90, DUR 90, BAR 98, ABG 94, VAN 93]. These methods can be viewed abstractly in the following operator composition form for a first-order conservation law in d space dimensions and time

$$u_0^{n+1} = A \cdot E(\tau) \cdot R_p^0(\cdot) u_0^n \tag{1}$$

where u_0^n are the piecewise constant cell-averages of the conservation law solution $u(x,t)$ at time t_n, $R_p^0(x)$ is a reconstruction operator which produces a cell-wise discontinuous p-th order polynomial approximation of the solution given cell-averages, $E(t)$ is the evolution operator for the PDE (including boundary conditions), and A is the cell-averaging operator such that $A|_K$ performs cell-averaging for each partition element K in the mesh $\mathcal{K}$. Since A is a positive operator and $E(\tau)$ represents exact evolution in the small, the control of solution oscillations and Gibbs-like phenomena is linked directly to oscillation properties of the reconstruction operator, $R_p^0(x)$. The requirements of high order accuracy for smooth solutions and discrete conservation give rise to the following additional design criterion for the reconstruction operator (see Harten [HAR 87, HAR 89])

- $R(x)u_0 = u(x) + O(h^{p+1})$ whenever u is smooth (2)
- $A|_K R(x)u_0 = u_0|_K, \ \forall K \in \mathcal{K}$ to insure discrete conservation (3)

A rather large body of literature exists devoted to the intricate design and analysis of various non-oscillatory reconstruction operators for Godunov finite volume methods. Perhaps surprisingly, we will show that an exact error representation formula and simple *a posteriori* error estimation theory can be

developed without knowing the precise details of a particular reconstruction operator beyond the requirements of Eqns. (2) and (3). This task is undertaken in the remainder of this article.

In developing the present *a posteriori* error estimation theory for finite volume methods, we will utilize the notion of a mesh dependent *broken space* $\mathcal{V}_p^{\mathrm{B}}$ consisting of discontinuous piecewise polynomials of at most degree p in each partition element. Using this space, we consider the Discontinuous Galerkin (DG) finite element method introduced by Reed and Hill [REE 73] as analyzed by Johnson and Pitkäranta [JOH 86] and further refined for nonlinear conservation laws by Cockburn et al. [COC 89, COC 97]:

DG FEM. Find $u_p \in \mathcal{V}_p^{\mathrm{B}}$ such that

$$\mathcal{B}_{\mathrm{DG}}(u_p, v) = F(v), \quad \forall v \in \mathcal{V}_p^{\mathrm{B}} \tag{4}$$

where $\mathcal{B}_{\mathrm{DG}}(\cdot,\cdot)$ denotes an abstract variational form corresponding to a weak integrated-by-parts form of the conservation law and $F(v)$ a functional possibly including boundary conditions and any external forcing terms. Precise forms of these operators will be given later. It is well-known that in the case $p = 0$, the DG method reduces to the lowest order accurate Godunov method. As will be shown later, the underpinning of our error estimation theory comes from the simple observation that the higher order Godunov methods can be expressed as a Petrov-Galerkin variant of the basic DG method:

Higher Order Godunov FVM. Find $u_0 \in \mathcal{V}_0^{\mathrm{B}}$ such that

$$\mathcal{B}_{\mathrm{DG}}(R_p^0 u_0, v) = F(v), \quad \forall v \in \mathcal{V}_0^{\mathrm{B}}, \quad R_p^0 : \mathcal{V}_0^{\mathrm{B}} \mapsto \mathcal{V}_p^{\mathrm{B}} \ . \tag{5}$$

Here R_p^0 represents the same reconstruction operator described in previous paragraphs which maps one broken space into another. Using these constructions, we will show that the *a posteriori* error estimation theory previously developed for the DG method can be modified for use in higher order Godunov methods with a modicum of effort by appealing directly to the Petrov-Galerkin form given in Eqn. (5).

REMARK. — Note that we will *not* attempt an *a priori* analysis of the Petrov-Galerkin form (5). Such an analysis would depend critically on the precise form of reconstruction operator used. In addition, *a priori* theories (stability, accuracy, convergence) for higher order Godunov finite volume methods are typically carried out in more convenient non-energy norms, see Harten [HAR 83, HAR 87, HAR 89] and Kröner et al. [KRO 95, KRO 96]. We once again emphasize that unlike the *a priori* theory, an *a posteriori* error estimation theory based on Eqn. (5) can be performed without knowing the precise details of the particular reconstruction operator. Thus we are able to obtain a simple error estimation theory with a wide range of direct applicability.

REMARK. — Finally, we remark that although we include time dependent terms in portions of the presentation, in our final analysis as well as calculated numerical results, we consider only error estimates for steady-state solutions.

2. Higher Order Godunov Finite Volume Methods in Petrov-Galerkin Form

Let Ω be a domain in $\mathbf{R}^d$ and $\mathcal{K}$ a partition of Ω into shape regular partition elements or control volumes, K. Further let $\mathcal{V}^{\mathrm{B}}$ be the mesh dependent broken space of discontinuous piecewise H^s functions defined on $\mathcal{K}$, i.e.,

$$\mathcal{V}^{\mathrm{B}} = \{v \,:\, v|_K \in H^s(K)\} \ . \tag{6}$$

Similarly, we introduce the finite dimensional spaces $\mathcal{V}_p^{\mathrm{B}}$ consisting of discontinuous piecewise polynomial functions of degree p defined on the partition $\mathcal{K}$

$$\mathcal{V}_p^{\mathrm{B}} = \{v \,:\, v|_K \in \mathcal{P}_p(K)\} \tag{7}$$

with $\mathcal{P}_p(K)$ the space of polynomials of degree $\leq p$ defined on element K.

Next consider the following prototype scalar nonlinear conservation law in a domain Ω with boundary Γ with solution $u(x,t) : \Omega \times \mathbf{R} \mapsto \mathbf{R}$ and flux vector $\vec{f}(u) : \mathbf{R} \mapsto \mathbf{R}^d$

$$\begin{array}{rcll} u_{,t} + \mathrm{div}\vec{f}(u) & = & 0, & \text{in } \Omega \times [0,T] \\ u(x,0) & = & u_0(x), & \text{in } \Omega \\ a^-(n;u)(g-u) & = & 0, & \text{on } \Gamma \ \text{ with } a(n;u) \equiv f_{,u} \cdot n \ . \end{array}$$

Let I_n denote the time slab increment, $I_n \equiv [t_n, t_{n+1}]$, with $[0,T] = \cup_{n=0,N-1} I_n$. In addition, let K and K' denote two partition elements adjacent to an edge e so that $u_\pm(\partial K \cap e)$ denotes the trace restrictions of functions on that edge segment such that $u_-(x)$ is the restriction from K and $u_+(x)$ is the restriction from K' for $x \in e$. Using this compact notation, the Godunov finite volume method and discontinuous Galerkin method for a single time slab increment are written succinctly as

Godunov Finite Volume. Find $u_0 \in \mathcal{V}_0^{\mathrm{B}}$ such that for each $K \in \mathcal{K}$

$$\frac{d}{dt}\int_{I_n} u_0|_K \, dt + \int_{I_n \times \partial K \setminus \Gamma} h(n; (R_p^0 u_0)_-, (R_p^0 u_0)_+) \, ds \, dt + \int_{I_n \times \partial K \cap \Gamma} h(n; (R_p^0 u_0)_-, g) \, ds \, dt = 0 \tag{8}$$

Discontinuous Galerkin. Find $u_p \in \mathcal{V}_p^{\mathrm{B}}$ for all $v \in \mathcal{V}_p^{\mathrm{B}}$ (implied sum on i)

$$\sum_{K \in \mathcal{K}} \Big(\int_{I_n \times K} v \ (u_p)_{,t} \, dx \, dt - \int_{I_n \times K} v_{,x_i} \ f^i(u_p) \, dx \, dt + \int_{I_n \times \partial K \setminus \Gamma} v_- \, h(n; (u_p)_-, (u_p)_+) \, ds \, dt + \int_{I_n \times \partial K \cap \Gamma} v_- \, h(n; (u_p)_-, g) \, ds \, dt \Big) = 0 \tag{9}$$

where $h(n; u_-, u_+)$ is a numerical flux function such that $\vec{f}(u) \cdot n = h(n; u, u)$ and $h(n; u_-, u_+) = -h(-n; u_+, u_-)$. In these formulations we have omitted (for sake of simplicity) those terms that would arise from discontinuous *in time* approximation since our final objective are error estimates at steady-state. Also observe that Eqn. (9) is consistent with our abstract variational representation given earlier for DG in Eqn. (4)

Find $u_p \in \mathcal{V}_p^{\mathrm{B}}$ *such that*

$$\mathcal{B}_{\mathrm{DG}}(u_p, v) = F(v), \quad \forall v \in \mathcal{V}_p^{\mathrm{B}} \ . \tag{10}$$

Close comparison of Eqns. (8) and (9) suggests the following lemma of importance in *a posteriori* error estimation for Godunov finite volume methods.

Lemma 2.1 *Let* R_p^0 *denote a reconstruction operator* $R_p^0 : \mathcal{V}_0^{\mathrm{B}} \mapsto \mathcal{V}_p^{\mathrm{B}}$ *on a nondeforming space-time partition* $\mathcal{K} \times I_n$ *satisfying the cell-averaging condition for* $u_0 \in \mathcal{V}_0^{\mathrm{B}}$ *and all* $K \in \mathcal{K}$

$$(R_p^0 u_0, v)|_K = (u_0, v)|_K, \quad \forall v \in \mathcal{V}_0^{\mathrm{B}} \tag{11}$$

where $(\cdot, \cdot)|_K$ *denotes an inner product integration on* Ω *restricted to a partition element* K*. The Godunov finite volume method (8) is written equivalently as the following Petrov-Galerkin variant of the discontinuous Galerkin method (9):*

Find $u_0 \in \mathcal{V}_0^{\mathrm{B}}$

$$\mathcal{B}_{\mathrm{DG}}(R_p^0 u_0, v) = F(v), \quad \forall v \in \mathcal{V}_0^{\mathrm{B}} \ . \tag{12}$$

Proof The proof follows immediately from term-by-term inspection of Eqns. (8) and (9) together with the cell-averaging condition (11). ∎

Observe that the cell-averaging condition given here in Eqn. (11) is identical to that given earlier in Eqn. (3).

3. *A Posteriori* Error Estimation of Functionals

Using lemma 2.1, an exact error representation formula and computable *a posteriori* error estimates will be derived for user specified functionals tailored to Godunov finite volume methods. The development given here follows closely the previous work of Becker and Rannacher [BEC 98] and Süli [Sul 98] as well as previous *a posteriori* error estimation work by the present authors [BAR 99, BAR 99b] for the DG method.

3.1. *Functionals*

The objective is to estimate the error in a user specified functional $M(u)$ which can be expressed as a weighted integration over the domain Ω

$$M_\psi(u) = \int_\Omega \psi \, N(u) \, dx$$

or a weighted integration on the boundary Γ

$$M_\psi(u) = \int_\Gamma \psi\, N(u)\, dx$$

for some user specified ψ and function $N(u) : \mathbf{R} \mapsto \mathbf{R}$. Examples of functionals used in later calculations are:

Example 1: Outflow functional, $u_{,t} + \lambda \cdot \nabla u = 0$

$$M_\psi(u) = \int_\Gamma \psi\, (\lambda \cdot n)^+\, u\, dx, \quad x \in \mathbf{R}^d \ . \tag{13}$$

Example 2: Solution average functional

$$M_{\text{ave}}(u) = \int_\Omega u\, dx, \quad x \in \mathbf{R}^d \ . \tag{14}$$

Example 3: Mollified pointwise functional

$$M_\psi(u) = \int_\Omega \psi(r_0; |x - x_0|)\, u\, dx, \quad x \in \mathbf{R}^2 \tag{15}$$

$$\psi(r_0; r) = \begin{cases} 0 & r \geq r_0 \\ \frac{e^{1/(r^2/r_0^2 - 1)}}{2\pi \int_0^{r_0} e^{1/(\xi^2/r_0^2 - 1)} \xi\, d\xi} & r < r_0 \end{cases} \ .$$

3.2. *Error Representation Formulas*

In this section, exact error representation formulas are derived for three abstract formulations with

(1) $B(\cdot, \cdot)$ a bilinear form with $M(\cdot)$ a linear functional

(2) $\mathcal{B}(\cdot, \cdot)$ a nonlinear variational form (nonlinear in the first argument and linear in the second argument) with $\mathcal{M}(\cdot)$ a nonlinear functional

(3) $\mathcal{B}(R_p^0 \cdot, \cdot)$ a nonlinear variational form (nonlinear in the first argument and linear in the second argument) with $\mathcal{M}(\cdot)$ a nonlinear functional

In these derivations, π_p denotes any suitable projection operator (e.g. interpolation, L_2 projection) into $\mathcal{V}_p^{\text{B}}$.

Error Representation: linear case. $B(\cdot, \cdot)$ and $M(\cdot)$ are both assumed linear.

Consider the primal numerical problem

Find $u_p \in \mathcal{V}_p^{\text{B}}$ *such that*

$$B(u_p, v) = F(v) \quad \forall\ v \in \mathcal{V}_p^{\text{B}}$$

with the Galerkin orthogonality property

$$B(u - u_p, v) = 0 \quad \forall\ v \in \mathcal{V}_p^{\mathrm{B}}$$

and introduce the auxiliary dual problem

Find $\Phi \in \mathcal{V}^{\mathrm{B}}$ *such that*

$$B(v, \Phi) = M(v) \quad \forall\ v \in \mathcal{V}^{\mathrm{B}} \ .$$

An exact error representation formula for a given functional $M(\cdot)$ results from the following steps

$$\begin{aligned}
M(u) - M(u_p) &= M(u - u_p) && \text{(linearity of } M\text{)} \\
&= B(u - u_p, \Phi) && \text{(dual problem)} \\
&= B(u - u_p, \Phi - \pi_p \Phi) && \text{(orthogonality)} \\
&= B(u, \Phi - \pi_p \Phi) - B(u_p, \Phi - \pi_p \Phi) && \text{(linearity of } B\text{)} \\
&= F(\Phi - \pi_p \Phi) - B(u_p, \Phi - \pi_p \Phi) && \text{(variational problem)}
\end{aligned}$$

thus yielding the simple exact error representation formula

$$M(u) - M(u_p) = F(\Phi - \pi_p \Phi) - B(u_p, \Phi - \pi_p \Phi) \ . \tag{16}$$

Error Representation: nonlinear case. $\mathcal{B}(\cdot, \cdot)$ and $\mathcal{M}(\cdot)$ are both nonlinear.

To cope with nonlinearity, we first introduce the mean-value linearizations

$$\begin{aligned}
\mathcal{B}(u, v) &= \mathcal{B}(u_p, v) + \overline{\mathcal{B}}(u_p, u; u - u_p, v) \quad \forall\ v \in \mathcal{V}^{\mathrm{B}} \\
\mathcal{M}(u) &= \mathcal{M}(u_p) + \overline{\mathcal{M}}(u_p, u; u - u_p) \ .
\end{aligned}$$

For example, if $\mathcal{B}(u, v) = (Lu, v)$ for some nonlinear differential operator L then for $v \in \mathcal{V}^{\mathrm{B}}$

$$\begin{aligned}
\mathcal{B}(u, v) &= \mathcal{B}(u_p, v) + \Big(\int_0^1 L_{,u}(\tilde{u}(\theta))\, d\,\theta\ (u - u_p), v \Big) \\
&= \mathcal{B}(u_p, v) + (\overline{L}_{,u}\,(u - u_p), v) \\
&= \mathcal{B}(u_p, v) + \overline{\mathcal{B}}(u_p, u; u - u_p, v).
\end{aligned}$$

with $\tilde{u}(\theta) \equiv u_p + (u - u_p)\ \theta$. Consider the nonlinear primal numerical problem

Find $u_p \in \mathcal{V}_p^{\mathrm{B}}$ *such that*

$$\mathcal{B}(u_p, v) = F(v) \quad \forall\ v \in \mathcal{V}_p^{\mathrm{B}} \tag{17}$$

with the orthogonality property

$$\overline{\mathcal{B}}(u_p, u; u - u_p, v) = 0 \quad \forall\ v \in \mathcal{V}_p^{\mathrm{B}}$$

and introduce the auxiliary linearized dual problem

Find $\Phi \in \mathcal{V}^{\mathrm{B}}$ *such that*

$$\overline{\mathcal{B}}(u_p, u; v, \Phi) = \overline{\mathcal{M}}(u_p, u; v) \quad \forall\ v \in \mathcal{V}^{\mathrm{B}} \ . \tag{18}$$

An exact error representation formula for a given nonlinear functional $\mathcal{M}(\cdot)$ then results from the following steps

$$\begin{aligned}
\mathcal{M}(u) - \mathcal{M}(u_p) &= \overline{\mathcal{M}}(u_p, u; u - u_p) && \text{(mean-value } \mathcal{M}\text{)} \\
&= \overline{\mathcal{B}}(u_p, u; u - u_p, \Phi) && \text{(dual problem)} \\
&= \overline{\mathcal{B}}(u_p, u; u - u_p, \Phi - \pi_p\Phi) && \text{(orthogonality)} \\
&= \mathcal{B}(u, \Phi - \pi_p\Phi) - \mathcal{B}(u_p, \Phi - \pi_p\Phi) && \text{(mean-value } \mathcal{B}\text{)} \\
&= F(\Phi - \pi_p\Phi) - \mathcal{B}(u_p, \Phi - \pi_p\Phi), && \text{(variational problem)}
\end{aligned}$$

thus yielding the following exact error representation formula

$$\mathcal{M}(u) - \mathcal{M}(u_p) = F(\Phi - \pi_p\Phi) - \mathcal{B}(u_p, \Phi - \pi_p\Phi) \ . \tag{19}$$

Note that although Eqns. (16) and (19) appear identical, mean-value linearization introduces a subtle right-hand side dependency on the exact solution in Eqn. (19). This complication is addressed in Sect. 4.2.

Error Representation: Godunov FVM Case. $\mathcal{B}(R_p^0\cdot, \cdot)$ and $\mathcal{M}(\cdot)$ are both nonlinear. Mean-value linearizations are again introduced as in the previous case

$$\begin{aligned}
\mathcal{B}(u, v) &= \mathcal{B}(R_p^0 u_0, v) + \overline{\mathcal{B}}(R_0^p u_0, u; u - R_p^0 u_0, v) \quad \forall\ v \in \mathcal{V}^{\mathrm{B}} \\
\mathcal{M}(u) &= \mathcal{M}(R_p^0 u_0) + \overline{\mathcal{M}}(R_p^0 u_0, u; u - R_p^0 u_0) \ .
\end{aligned}$$

Consider the primal Godunov FVM problem

Find $u_0 \in \mathcal{V}_0^{\mathrm{B}}$ *such that*

$$\mathcal{B}(R_p^0 u_0, v) = F(v) \quad \forall\ v \in \mathcal{V}_0^{\mathrm{B}} \tag{20}$$

with the orthogonality property

$$\overline{\mathcal{B}}(R_p^0 u_0, u; u - R_p^0 u_0, v) = 0 \quad \forall\ v \in \mathcal{V}_0^{\mathrm{B}}$$

and introduce the auxiliary linearized dual problem

Find $\Phi \in \mathcal{V}^{\mathrm{B}}$ *such that*

$$\overline{\mathcal{B}}(R_p^0 u_0, u; v, \Phi) = \overline{\mathcal{M}}(v) \quad \forall\ v \in \mathcal{V}^{\mathrm{B}}. \tag{21}$$

An exact error representation formula for a given nonlinear functional $\mathcal{M}(\cdot)$ for the class of Godunov finite volume methods results from the following steps

$$\begin{aligned}
\mathcal{M}(u) - \mathcal{M}(R_p^0 u_0) &= \overline{\mathcal{M}}(u - R_p^0 u_0) && \text{(mean-value } \mathcal{M}) \\
&= \overline{\mathcal{B}}(u - R_p^0 u_0, \Phi) && \text{(dual problem)} \\
&= \overline{\mathcal{B}}(u - R_p^0 u_0, \Phi - \pi_0 \Phi) && \text{(orthogonality)} \\
&= \mathcal{B}(u, \Phi - \pi_0 \Phi) - \mathcal{B}(R_p^0 u_0, \Phi - \pi_0 \Phi) && \text{(mean-value } \mathcal{B}) \\
&= F(\Phi - \pi_0 \Phi) - \mathcal{B}(R_p^0 u_0, \Phi - \pi_0 \Phi), && \text{(variational problem)}
\end{aligned}$$

thus yielding the following exact error representation formula

$$\mathcal{M}(u) - \mathcal{M}(R_p^0 u_0) = F(\Phi - \pi_0 \Phi) - \mathcal{B}(R_p^0 u_0, \Phi - \pi_0 \Phi) \ . \tag{22}$$

This final form for the Godunov finite volume method serves as a progenitor for the remaining derivations given below.

4. Computable Error Estimates

Computationally, the error representation formulas (16), (19) and (22) are not suitable for obtaining computable *a posteriori* error estimates and use in mesh adaptation.

• $\Phi \in \mathcal{V}^B$, the solution of the infinite dimensional problem is not generally known.

• The mean-value linearization used in the linearized dual problems (18) and (21) requires knowledge of the exact solution u.

• The error representation formulas do not suggest any simple strategy for element refinement/coarsening.

4.1. *Approximating* $\Phi - \pi_0 \Phi$

We list several strategies for approximating $\Phi - \pi_0 \Phi$ for Godunov finite volume methods. The first two techniques seek to exploit the two scale structure of Godunov methods, i.e. that as a weighted residual method of Petrov-Galerkin type, the residual is orthogonal to test functions in $\mathcal{V}_0^{\mathrm{B}}$ and not to test functions in $\mathcal{V}_p^{\mathrm{B}}$.

Inherent two scale approximation. Compute the linearized dual problem:

Find $\Phi_0 \in \mathcal{V}_0^{\mathrm{B}}$ *such that*

$$\overline{\mathcal{B}}(R_p^0 u_0, u; v, R_p^0 \Phi_0) = \overline{\mathcal{M}}(R_p^0 u_0, u; v), \quad \forall\, v \in \mathcal{V}_0^{\mathrm{B}}$$

and approximate

$$\Phi - \pi_0 \Phi \approx R_p^0 \Phi_0 - \Phi_0 \ . \tag{23}$$

REMARK. — This strategy fails in standard Galerkin finite element methods since any approximation of $\Phi \in \mathcal{V}_p^{\mathrm{B}}$ is orthogonal to the residual, hence with Galerkin finite element methods the contribution is identically zero and no error estimate is obtained.

Patch recovery post-processing. Compute the linearized dual problem:

Find $\Phi_0 \in \mathcal{V}_0^{\mathrm{B}}$ *such that*

$$\overline{\mathcal{B}}(R_p^0 u_0, u; v, R_p^0 \Phi_0) = \overline{\mathcal{M}}(R_p^0 u_0, u; v), \quad \forall\, v \in \mathcal{V}_0^{\mathrm{B}}$$

and approximate using a patch recovery technique $\overline{R}_q^p : \mathcal{V}_p^{\mathrm{B}} \mapsto \mathcal{V}_q^{\mathrm{B}}$ for $q \geq p$

$$\Phi - \pi_0 \Phi \approx \overline{R}_q^p R_p^0 \Phi_0 - \Phi_0 \ . \tag{24}$$

The patch recovery is motivated by the original work of Zienkiewicz and Zhu [ZIE 92]. In the present computations, the least squares reconstruction operator discussed in Section 6 is also used as a patch recovery operator so that

$$\overline{R}_q^p R_p^0 u_0 = R_q^0 u_0 \ . \tag{25}$$

Global higher order solves. Solve the linearized dual problem global using a higher order method:

Find $\Phi_0 \in \mathcal{V}_0^{\mathrm{B}}$ *such that*

$$\overline{\mathcal{B}}(R_p^0 u_0, u; v, R_q^0 \Phi_0) = \overline{\mathcal{M}}(R_p^0 u_0, u; v), \quad \forall\, v \in \mathcal{V}_0^{\mathrm{B}}$$

for some $q > p$. While conceptually straightforward, this technique typically makes solving the linearized dual problem more computationally expensive than the primal problem in terms of computer memory and arithmetic operations. This can be prohibitive in three space dimensions.

4.2. *Approximating the Mean-value Linearized Dual Problem*

The mean-value linearization requires knowledge of the exact solution u. Two computable approximate linearizations are considered

Jacobian derivative linearization. The mean-value linearization is supplanted by the Jacobian linearization so that the computable linearized dual problem for the Godunov method is obtained

Find $\Phi_0 \in \mathcal{V}_0^{\mathrm{B}}$ *such that*

$$\overline{\mathcal{B}}(R_p^0 u_0, R_p^0 u_0; v, \Phi_0) = \overline{M}(R_p^0 u_0, R_p^0 u_0; v) \quad \forall\ v \in \mathcal{V}^{\mathrm{B}}.$$

This strategy is used in all subsequent numerical calculations.

Mean-value linearization via post-processing and numerical quadrature. The Godunov method provides easy access to post-processed approximations of the solution, i.e. $\overline{R}_q^p R_p^0 u_0$ as $R_q^0 u_0$ for $q > p$, thus suggesting the improved computable approximation of the mean-value linearized dual problem

Find $\Phi_0 \in \mathcal{V}_0^{\mathrm{B}}$ *such that for* $q > p$

$$\overline{\mathcal{B}}(R_p^0 u_0, R_q^0 u_0; v, \Phi_0) = \overline{M}(R_p^0 u_0, R_q^0 u_0; v) \quad \forall\ v \in \mathcal{V}^{\mathrm{B}}.$$

where numerical quadrature could be employed to approximate the mean-value path integration.

4.3. *Direct Estimates*

Given the error representation formula (22) for the Godunov finite volume method, error estimates suitable for adaptive meshing are easily obtained

$$\begin{aligned}
|\mathcal{M}(u) - \mathcal{M}(R_p^0 u_0)| &= \left|\mathcal{B}(R_p^0 u_0, \Phi - \pi_0\Phi) - F(\Phi - \pi_0\Phi)\right| \quad \text{(error representation)} \\
&= |\sum_{K\in\mathcal{K}} \big(\mathcal{B}_K(R_p^0 u_0, \Phi - \pi_0\Phi) - F_K(\Phi - \pi_0\Phi)\big)| \qquad \text{(element assembly)} \\
&\le \sum_{K\in\mathcal{K}} \left|\big(\mathcal{B}_K(R_p^0 u_0, \Phi - \pi_0\Phi) - F_K(\Phi - \pi_0\Phi)\big)\right| \quad \text{(triangle inequality)}
\end{aligned} \tag{26}$$

where $\mathcal{B}_K(\cdot,\cdot)$ and $F_K(\cdot)$ are restrictions of $\mathcal{B}(\cdot,\cdot)$ and $F(\cdot)$ to the partition element K.

Note that the element assembly representation is not unique. For example strong and weak forms of the variational operator $\mathcal{B}(\cdot,\cdot)$ yield differing assembly representations. For the Godunov finite volume method with time terms omitted, the error representation formula (22) yields

$$\begin{aligned}
\mathcal{B}(R_p^0 u_0, \Phi - \pi_0\Phi) - F(\Phi - \pi_0\Phi) = \sum_{K\in\mathcal{K}} \Big(&- \int_K \vec{f}^{\,i}(R_p^0 u_0)\,(\Phi - \pi_0\Phi)_{,x_i}\,dx \\
&+ \int_{\partial K\setminus\Gamma} (\Phi - \pi_0\Phi)_-\, h(n; (R_p^0 u_0)_-, (R_p^0 u_0)_+)\,ds \\
&+ \int_{\partial K\cap\Gamma} (\Phi - \pi_0\Phi)_-\, h(n; (R_p^0 u_0)_-, g)\,ds\Big).
\end{aligned} \tag{27}$$

The present numerical computations utilize the numerical flux formula

$$h(n; u_-, u_+) = \frac{1}{2}\left(f(n; u_-) + f(n; u_+)\right) - \frac{1}{2}|a(n; \overline{u}(u_-, u_+))|\,[u]_-^+ \tag{28}$$

with $\overline{u}(u_-, u_+)$ chosen so that

$$[f(n;u)]_-^+ = a(n; \overline{u}(u_-, u_+))\,[u]_-^+ \tag{29}$$

with $f(n;u) = (\vec{f}(u_-) \cdot n)$ and $a(n;u) = \partial f(n;u)/\partial u$. Using this particular numerical flux, the following weighted residual (strong) form can be obtained upon integration by parts

$$\begin{aligned}\mathcal{B}(R_p^0 u_0, \Phi - \pi_0\Phi) - F(\Phi - \pi_0\Phi) = \sum_{K\in\mathcal{K}} \Big(& \int_K (\Phi - \pi_0\Phi)\ \mathrm{div}\vec{f}(R_p^0 u_0)\, dx \\ & + \int_{\partial K\setminus\Gamma} (\Phi - \pi_0\Phi)_-\, a^-(n; (R_p^0 u_0)_-, (R_p^0 u_0)_+)\, [R_p^0 u_0]_-^+\, ds \\ & + \int_{\partial K\cap\Gamma} (\Phi - \pi_0\Phi)_-\, a^-(n; (R_p^0 u_0)_-, g)\, (g - (R_p^0 u_0)_-)\, ds \Big). \quad (30)\end{aligned}$$

This latter weighted residual form and the implied element assembly form $\sum_K \mathcal{B}_K(\cdot,\cdot) - F_K(\cdot)$ is preferred in the error estimates (26) since the individual terms represent residual components that vanish individually when the exact solution is inserted into the variational form and a slightly sharper approximation is obtained after application of the triangle inequality in (26).

5. Adaptive Meshing

The error estimates of the previous section motivate a simple strategy for mesh adaptation. Defining for each partition element K

$$\eta_K \equiv \mathcal{B}_K(R_p^0 u_0, \Phi - \pi_0\Phi) - F_K(\Phi - \pi_0\Phi) \quad (31)$$

we have a candidate *adaptation element indicator* $|\eta_K|$ such that

$$\left|\mathcal{M}(u) - \mathcal{M}(R_p^0 u_0)\right| \le \sum_{K\in\mathcal{K}} |\eta_K| \quad (32)$$

and an accurate *adaptation stopping criteria*

$$\left|\mathcal{M}(u) - \mathcal{M}(R_p^0 u_0)\right| = |\sum_{K\in\mathcal{K}} \eta_K| \ . \quad (33)$$

These quantities suggest a simple mesh adaptation strategy in common use with other indicator functions:

Mesh Adaptation Algorithm

(1) Construct an initial mesh $\mathcal{K}$.

(2) Compute a numerical approximation of the primal problem on the current mesh $\mathcal{K}$ using Godunov's method with p-th order reconstruction yielding $R_p^0 u_0$.

(3) Compute a numerical approximation of the dual problem on the current mesh $\mathcal{K}$ using Godunov's method with p-th order reconstruction yielding $R_p^0 \Phi_0$.

(4) Optionally improve the accuracy of the numerically computed dual problem via a post-processing recovery operator $\overline{R}_q^p$ for $q \ge p$ yielding $\overline{R}_q^p R_p^0 \Phi_0$.

(5) Compute η_K for all elements in $\mathcal{K}$ using $R_p^0 u_0$ and the approximation

$$\Phi - \pi_0 \Phi \approx R_p^0 \Phi_0 - \Phi_0 \quad \text{or} \quad \Phi - \pi_0 \Phi \approx \overline{R}_q^p R_p^0 \Phi_0 - \Phi_0 \ .$$

(6) If($|\sum_{K\in\mathcal{K}} \eta_K| < TOL$) STOP

(7) Otherwise, refine and coarsen a user specified fraction of the total number of elements according to the size of $|\eta|_K$, generate a new mesh $\mathcal{K}$ and GOTO 2

6. Least Squares Reconstruction on Patches

The reconstruction operator used in calculations is based on a least squares approximation given cell-averages on patches of elements. Let $\mathcal{N}(K) \subset \Omega$ denote a patch of elements containing the element K. The global reconstruction operator $R_p^0 : \mathcal{V}_0^{\mathrm{B}} \to \mathcal{V}_p^{\mathrm{B}}$ is constructed piecewise on a local patch-by-patch basis with

$$(R_{p,\mathcal{N}(K)}^0 u_0)|_K = (R_p^0 u_0)|_K, \quad \forall K \in \mathcal{K}$$

for $u_0 \in \mathcal{V}_0^{\mathrm{B}}$ so that the task reduces to that of finding the local patch reconstruction operator $R_{p,\mathcal{N}(K)}^0$ for each $K \in \mathcal{K}$. To do so, first define the L_2 projection $\Pi_0 : \mathcal{V}^{\mathrm{B}} \mapsto \mathcal{V}_0^{\mathrm{B}}$, i.e. for each $u \in \mathcal{V}^{\mathrm{B}}$

$$(u - \Pi_0 u, v) = 0, \quad \forall v \in \mathcal{V}_0^{\mathrm{B}} \ .$$

The local reconstruction operator $R_{p,\mathcal{N}(K)}^0$ is then constructed from the following two conditions

1) **Exact Π_0 projection in element K.** The $\Pi_{0,K}$ projection of $R_{p,\mathcal{N}(K)}^0 u_0$ is exact in element K, i.e., it holds that

$$\Pi_{0,K} R_{p,\mathcal{N}(K)}^0 u_0 = u_{0,K} \quad \text{for each } u_0 \in \mathcal{V}_0^{\mathrm{B}}. \tag{34}$$

where $\Pi_{0,K}$ and $u_{0,K}$ denote restrictions of Π_0 and u_0 to the element K. This condition is equivalent to the cell-averaging property given in Eqn. (3).

2) **Constrained least squares fitting on patch $\mathcal{N}(K)$.** The L_2 deviation of the $\Pi_{0,K'}$ projection of $R_{p,\mathcal{N}(K)}^0 u_0$ from given cell-averaged data in patch elements $K' \in \mathcal{N}(K)$ is minimized subject to the constraint (34)

$$\|u_0 - \Pi_0 R_{p,\mathcal{N}(K)}^0 u_0\|_{\mathcal{N}(K)} = \min_{w \in \mathcal{Q}_p(\mathcal{N}(K))} \|u_0 - \Pi_0 w\|_{\mathcal{N}(K)}, \tag{35}$$

for all $u_0 \in \mathcal{V}_0^{\mathrm{B}}$. Here $\mathcal{Q}_p(\mathcal{N}(K))$ is the subspace of polynomials in $\mathcal{P}_p(\mathcal{N}(K))$ such that (34) holds.

Remark. — [p-th Order Exactness] Note that the patch cardinality card($\mathcal{N}(K)$) is always chosen sufficiently large (e.g. by increasing graph distance) so that there exists a unique solution to the constrained least squares problem and the local reconstruction operator $R_{p,\mathcal{N}(K)}^0$ is fully determined. As a consequence, it follows that for $r \leq p$

$$R_{p,\mathcal{N}(K)}^0 \Pi_0 u_r = u_r \quad \forall u_r \in \mathcal{P}_r(\mathcal{N}(K)),$$

which simply asserts that if the given data u_r is in the space of polynomials of degree $r \leq p$ in the patch neighborhood $\mathcal{N}(K)$, then the elementwise projection to cell-averages followed by p-th order patch reconstruction exactly reproduces the given data.

7. Slope Limiting for Discontinuous Solutions

For solutions containing discontinuities such as the Burgers' equation example of Sect. 8, a slope limiter is employed so that non-oscillatory solutions are obtained. The following particular solution ansatz for each $K \in \mathcal{K}$

$$U(x)_K \equiv u_{0,K} + \Psi_K \cdot (R_p^0(x)u_0 - u_0)_K, \quad x \in \mathbf{R}^d \tag{36}$$

is chosen with $\Psi_K \in [0,1]$ so that the cell-average property of the reconstruction (34) is maintained regardless of the particular value of Ψ_K. Next for each $K \in \mathcal{K}$ compute the minimum and maximum of all adjacent neighbor cell-averages

$$u_K^{\min} = \min_{K' \in \mathcal{N}(K)} u_{0,K'}, \quad u_K^{\max} = \max_{K' \in \mathcal{N}(K)} u_{0,K'}$$

and determine the largest value of $\Psi_K \in [0,1]$ such that

$$u_K^{\min} \leq U(x)_K \leq u_K^{\max}$$

when evaluated at the quadrature points used in the flux integral computation. To achieve this, compute the extrapolated state $U(x_q)$ at each quadrature point location x_q in the flux integral and determine the most restrictive Ψ_K

$$\Psi_K = \begin{cases} \min(1, \frac{u_K^{\max} - u_{0,K}}{U(x_q) - u_{0,K}}), & \text{if } U(x_q) - u_{0,K} > 0 \\ \min(1, \frac{u_K^{\min} - u_{0,K}}{U(x_q) - u_{0,K}}), & \text{if } U(x_q) - u_{0,K} < 0 \\ 1 & \text{if } U(x_q) - u_{0,K} = 0 \end{cases} \tag{37}$$

across all quadrature points. Unfortunately, the convergence of nonlinear iterative methods can be erratic using this type of non-differentiable limiter. Consequently, an additional quadratic dissipation term is added to the numerical flux function for discontinuous solution problems to enhance the convergence of nonlinear iterative methods

$$\begin{aligned} h^{\text{mod}}(n, \epsilon; (R_p^0 u_0)_-, (R_p^0 u_0)_+) &= h(n; (R_p^0 u_0)_-, (R_p^0 u_0)_+) \\ &+ \epsilon \sup_{\Omega} |\vec{f}'| \left(\frac{[R_p^0 u_0]_-^+}{[u_0]_-^+} \right)^2 [u_0]_-^+ \end{aligned} \tag{38}$$

with $\epsilon = .01$ used in the Burgers' equation calculations given below.

8. Numerical Results

To validate and assess the *a posteriori* error estimation theory for the Godunov finite volume method, numerical solutions for linear advection and nonlinear Burgers' equation are computed.

Linear Advection. $u(x,y) : [0,1]^2 \mapsto \mathbf{R}$ with $\lambda = (-y,x)^T$.

$$\begin{aligned} \mathrm{div}(\lambda\, u) &= 0, \quad \text{in } [0,1]^2 \\ u(x,0) &= g(x), \\ u(1,y) &= 0, \end{aligned}$$

with inflow profile data

$$g(x) = \begin{cases} \widetilde{\psi}(9/20; |x-1/2|) \cdot (1 - \widetilde{\psi}(9/20; |x-1/20|)) & \text{if } x \le 1/2 \\ \widetilde{\psi}(9/20; |x-1/2|) \cdot (1 - \widetilde{\psi}(9/20; |x-19/20|)) & \text{if } x > 1/2 \end{cases}$$

where $\widetilde{\psi}(r;x) \equiv \psi(r;x)/\psi(r;0)$ and $\psi(r;x)$ the mollifier function defined in Eqn. 15. Figure 1 (left) shows isocontours of the primal numerical solution obtained using the Godunov method with linear reconstruction on a relatively fine mesh containing 6400 elements. Figure 1 (right) graphs global measures

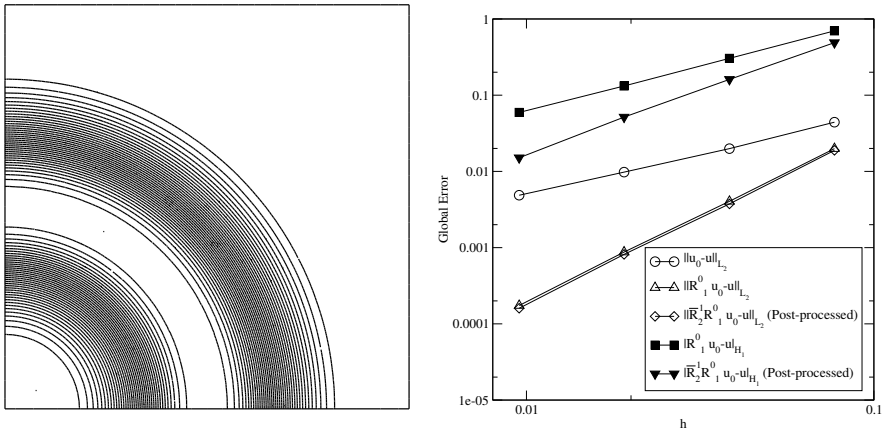


Figure 1. *Circular advection problem. Isocontours of the primal numerical solution $R_1^0 u_0$ computed using the Godunov FVM method with linear reconstruction on a mesh containing 6400 elements (left) and global measures of solution error versus mesh spacing parameter h (right).*

of the solution error on meshes containing 400, 1600, 6400 and 25600 elements. The graphs show that the L_2 solution error in cell-averages $\|u_0 - u\|_{L_2}$ as well as the H_1 semi-norm of the linearly reconstructed solution $|R_1^0 u_0 - u|_{H_1}$ are both first order accurate as expected while the L_2 solution error in the linearly reconstructed solution $\|R_1^0 u_0 - u\|_{L_2}$ exceeds second order accuracy. Also included in these graphs is the effect of solution post-processing. Specifically, the quadratic post-processing recovery procedure $\overline{R}_2^1 R_1^0 u_0 = R_2^0 u_0$ was employed. Although the L_2 norm $\|R_2^0 u_0 - u\|_{L_2}$ shows no improvement in convergence rate (slope), a slight vertical shift in the graph of this data indicates a slight improvement in absolute accuracy that is somewhat obfuscated by the logarithmic scaling. More conspicuous is the improvement in the H_1 semi-norm. The

effect of post-processing is to increase the convergence rate of $|R_2^0 u_0 - u|_{H_1}$ to second order. This indicates significant improvement in the accuracy of derivative information through least squares post-processing. This improvement is visually seen in Fig. 2 which shows isocontours of the numerical solution obtained on the coarsest mesh and the effect of quadratic post-processing. Next,

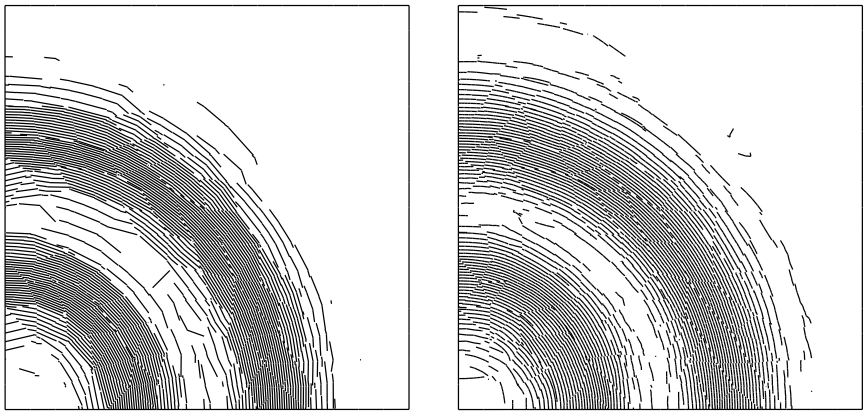


Figure 2. *Isocontours of the coarsest mesh (400 elements) numerical solution $R_1^0 u_0$ obtained using the Godunov FVM with linear reconstruction (left) and isocontours of the post-processed solution $\overline{R}_2^1 R_1^0 u_0 = R_2^0 u_0$ (right).*

the *a posteriori* error estimates are evaluated. Specifically considered are

- The outflow functional Eqn. (13) with

$$\psi_{\text{outflow}}(x,y) = \begin{cases} \widetilde{\psi}(7/20; |y-3/5|) \cdot (1 - \widetilde{\psi}(7/20; |y-1/4|)) & \text{if } y \le 3/5 \\ \widetilde{\psi}(7/20; |y-3/5|) \cdot (1 - \widetilde{\psi}(7/20; |y-19/20|)) & \text{if } y > 3/5 \end{cases} .$$

- The solution average functional Eqn. (14).
- The mollified pointwise value functional Eqn. (15) with

$$\psi_{\text{mollified}}(x,y) = \widetilde{\psi}(1/20; \sqrt{(x-1/10)^2 + (y-3/5)^2}) \ .$$

Dual solutions and error estimates are shown in Figs. 3-5. Each of these figures shows isocontours for the numerical solution of the dual problem (left) and graphs of the functional error and the *a posteriori* error estimates (right). The graphs in Figs. 3-5 each contain five curves. The first curve depicts the exact functional error $|\Delta M|$ since the analytic primal solution is known. Observe the third order superconvergence in the outflow functional and the mollified pointwise value functional. For each functional the continuous dual solution Φ can be constructed either exactly via Green's function or to a specified accuracy using series expansion and/or adaptive quadrature. Using this Φ, the second curve

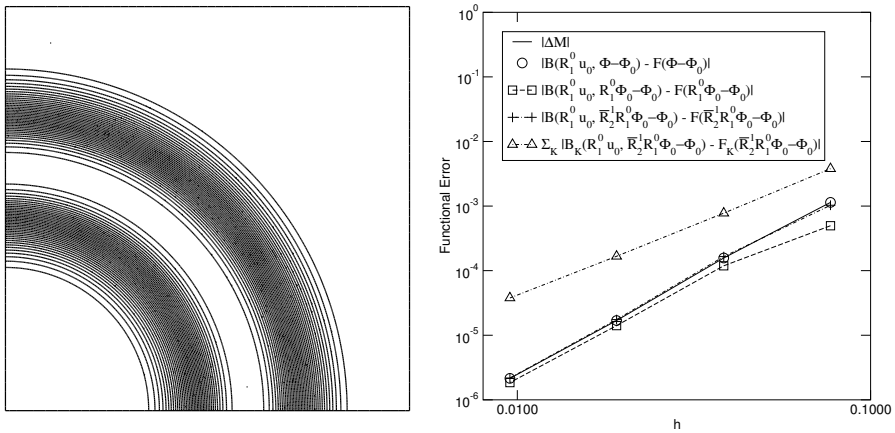


Figure 3. *Outflow functional for the pure advection problem using the Godunov FVM with linear reconstruction. Isocontours of the dual problem solution (left) and functional error versus mesh parameter h (right).*

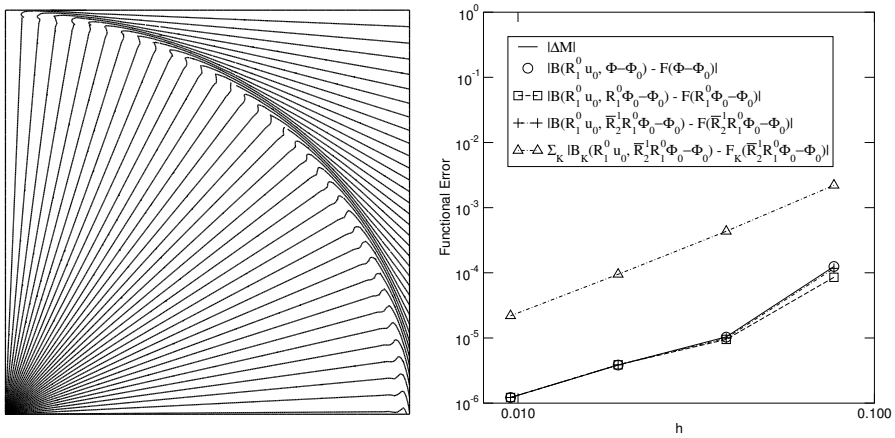


Figure 4. *Integral solution average functional for the pure advection problem using the Godunov FVM with linear reconstruction. Isocontours of the dual problem solution (left) and functional error versus mesh parameter h (right).*

depicts $|B(R_1^0 u_0, \Phi - \pi_0\Phi) - F(\Phi - \pi_0\Phi)|$ which according to (22) should be identical to the first curve $|\Delta M|$. This is verified for each functional. Curve number three graphs $|B(R_1^0 u_0, R_1^0\Phi_0 - \Phi_0) - F(R_1^0\Phi_0 - \Phi_0)|$ so that the effect of numerically approximating the continuous dual problem is assessed. Some noticable error is observed on coarse meshes but the performance on the finest meshes is quite acceptable. Curve number four shows the effect of post-processing of the numerically obtained dual data $|B(R_1^0 u_0, R_2^0\Phi_0 - \Phi_0) - F(R_2^0\Phi_0 - \Phi_0)|$.

Using this post-processed dual data, good accuracy is obtained on all meshes for all functionals except perhaps the mollified pointwise value functional. In this latter case, the dual solution consists of a slightly smoothed ridge function that is not well-resolved on the coarsest meshes using linear or quadratic approximations. Even so, the estimates in curves three or four seem acceptable as an adaptive mesh stopping criteria. Curve number five graphs

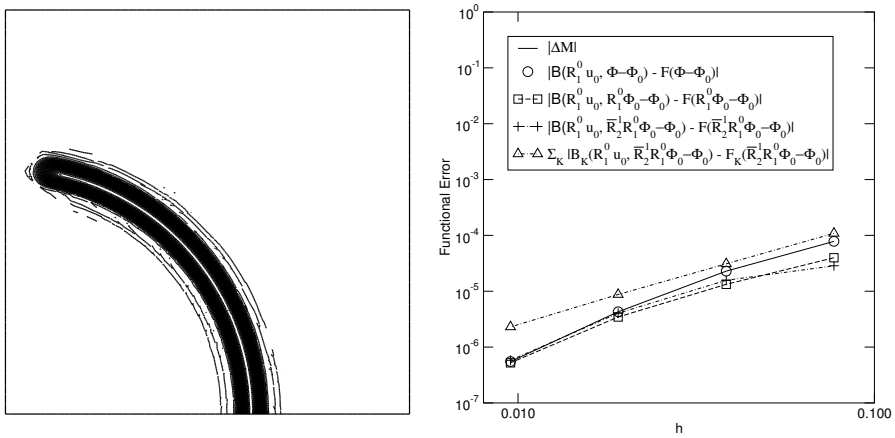
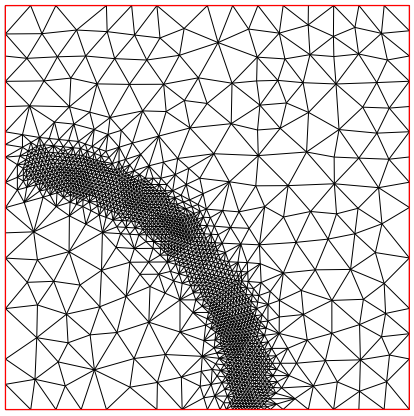


Figure 5. *Mollified pointwise value functional for the pure advection problem using the Godunov FVM with linear reconstruction. Isocontours of the dual problem solution (left) and functional error versus mesh parameter h (right).*



Adaptation Levels	#cells	$\lvert\Delta M\rvert$
0	400	1.9E-3
1	602	9.4E-4
2	1232	1.7E-5
3	3418	5.8E-8

Figure 6. *Adapted mesh for mollified pointwise value functional (left) and tabulated mesh sizes for increasing levels of refinement (right).*

$\sum_{K\in\mathcal{K}} |B_K(R_1^0 u_0, R_2^0\Phi_0 - \Phi_0) - F_K(R_2^0\Phi_0 - \Phi_0)|$ for each functional. In this approximation, interelement error cancellation does not occur because of the application of the triangle inequality in Eqn. (26). Consequently, the third

order superconvergence rates seen in the outflow and mollified functionals is absent and only second order rates of convergence are observed for all functionals. In addition, this last estimate over predicts the true error by factors of 3-1000 depending of the functional and the mesh size. Finally, in Fig. 6 (left) an adapted mesh obtained for the mollified pointwise value functional is plotted. The mesh has been adapted using the algorithm of Sect. 5 with quadratically post-processed numerical dual data. Figure 6 (right) indicates the efficiency of the adaptation procedure by tabulating levels of adaptation, mesh sizes, and the functional error for each level of adaptation.

Burgers' Equation. $u(x,y) : [0,1]^2 \mapsto \mathbf{R}$ with $\lambda = (u/2, 1)^T$.

$$\begin{aligned} \mathrm{div}(\lambda\, u) &= 0, \quad \text{in } [0,1]^2 \\ u(x,0) &= 5/4 - 2x, \\ u(1,y) &= -3/4, \\ u(0,y) &= 5/4 \ . \end{aligned}$$

As a final example, Burgers' equation is solved in a unit square as shown in

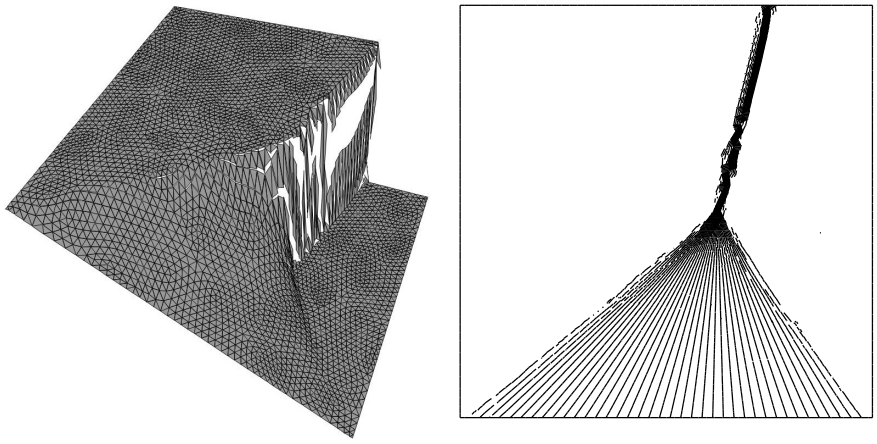


Figure 7. *Primal numerical solution $R_1^0 u_0$ for Burgers' equation problem using the Godunov FVM with linear reconstruction. Carpet plot in 3D (left) and solution isocontours in 2D (right).*

Fig. 7. As mentioned earlier, the Jacobian linearization is used as an approximation of the mean-value linearization for the dual problem. Unfortunately, the limiter function Ψ_K in Eqn. (36) is highly non-differentiable and has not been linearized in the present computations. For this problem, error estimates for the solution average functional Eqn. (14) have been obtained. Isocontours of the dual solution are shown in Fig. 8 (left). It is observed that monotonicity of the primal shock profile is essential for obtaining meaningful numerical approximations of the dual problem. Figure 8 (right) graphs the functional error using various approximations. The first curve graphs the exact functional error

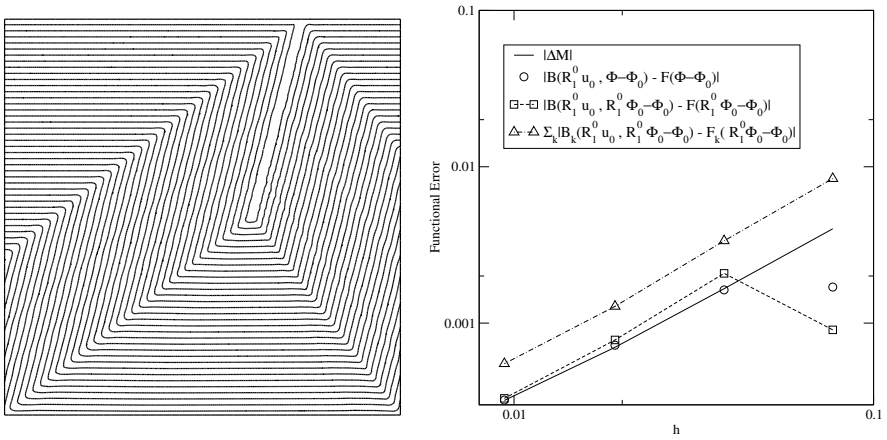


Figure 8. *Integral solution average functional for Burgers' equation problem. Isocontours of the dual problem (left) and functional error versus mesh spacing parameter h (right).*

$|\Delta M|$. Observe that this functional converges at a first order rate presumably due to the first order accuracy of the primal scheme in the shock region. The second curve graphs $|B(R_1^0 u_0, \Phi - \pi_0\Phi) - F(\Phi - \pi_0\Phi)|$ but using an analytical Φ linearized about the exact solution. Consequently, this quantity only approximates $|\Delta M|$ and large differences are seen on the coarsest mesh. The third curve graphs $|B(R_1^0 u_0, R_1^0\Phi_0 - \Phi_0) - F(R_1^0\Phi_0 - \Phi_0)|$ using a numerically approximated dual problem. Again large discrepancies are seen on the coarsest mesh. With mesh refinement the accuracy quickly becomes acceptable. Note we have not included post-processing of the dual data in these calculations. The fourth curve graphs $\sum_{K\in\mathcal{K}} |B_K(R_1^0 u_0, R_1^0\Phi_0 - \Phi_0) - F_K(R_1^0\Phi_0 - \Phi_0)|$. The results show that this estimate over predicts the true error by an order of magnitude but show the same rate of convergence as the true error.

These results give some evidence that the numerical approximations introduced due to nonlinearity become small under modest mesh refinement. Improved approximations for nonlinear problems are currently being pursued by the first author in related work applicable to both the discontinuous Galerkin and finite volume methods.

9. Concluding Remarks

A simple *a posteriori* error estimation theory for user specified functionals has been constructed that is tailored for higher order Godunov finite volume methods. Many issues remain unresolved:

• Mean-value linearization for schemes with non-differentiable limiters and/or reconstruction algorithms.

• Approximation of the infinite dimensional dual problem.

• Improved post-processing strategies.

Even so, the results presented here verify the abstract theory and suggest that further investigation is warranted.

References

[ABG 94] Abgrall, R., "An Essentially Non-Oscillatory Reconstruction Procedure on Finite-Element Type Meshes", *Comp. Meth. Appl. Mech. Engrg.*, vol. 116, 1994, pp. 95–101.

[BAR 98] Barth, T.J., "Numerical Methods for Gasdynamic Systems on Unstructured Meshes", in Kröner, Ohlberger, and Rohde, editors, *An Introduction to Recent Developments in Theory and Numerics for Conservation Laws*, of *Lecture Notes in Computational Science and Engineering*, Springer-Verlag Pub., Heidelberg, vol. 5, 1998, pp. 195–285.

[BAR 99] Barth, T.J., "Simplified Discontinuous Galerkin Methods for Systems of Conservation Laws with Convex Extension", in Cockburn, Karniadakis, and Shu, editors, *Discontinuous Galerkin Methods*, *Lecture Notes in Computational Science and Engineering*. Springer-Verlag, Heidelberg, vol. 11, 1999.

[BAR 02] Barth, T.J., Deconinck, H.(editors), *Error Estimation and Adaptive Discretization Methods for PDEs*, *Lecture Notes in Computational Science and Engineering*. Springer-Verlag, Heidelberg, vol. (in press) 2002.

[BAR 90] Barth, T.J., Frederickson. P.O.,"Higher Order Solution of the Euler Equations on Unstructured Grids Using Quadratic Reconstruction", Technical Report 90-0013, AIAA, Reno, NV, 1990.

[BAR 89] Barth, T.J., Jespersen, D.C., "The Design and Application of Upwind Schemes on Unstructured Meshes", Technical Report 89-0366, AIAA, Reno, NV, 1989.

[BAR 99b] Barth, T.J., Larson M.G., "A Posteriori Error Estimation for Adaptive Discontinuous Galerkin Approximations of Hyperbolic Systems", Technical Report NAS-99-010, NASA Ames Research Center, 1999.

[BEC 98] Becker, R., Rannacher, R., "Weighted A-Posteriori Error Control in FE Methods", in *Proc. ENUMATH-97, Heidelberg*. World Scientific Pub., Singapore, 1998.

[COC 89] Cockburn, B., Lin, S.Y., Shu, C.-W., "TVB Runge-Kutta Local Projection Discontinuous Galerkin Finite Element Method for Conservation Laws III: One Dimensional Systems", *J. Comp. Phys.*, vol. 84, 1989, pp. 90–113.

[COC 97] Cockburn, B., Shu, C.-W., "The Runge-Kutta Discontinuous Galerkin Method for Conservation Laws V: Multidimensional Systems", Technical Report 201737, ICASE, NASA Langley R.C., 1997.

[DUR 90] Durlofsky, L., Osher, S. Engquist, B., "Triangle Based TVD Schemes for Hyperbolic Conservation Laws", Technical Report 90-10, ICASE, NASA Langley R.C., 1990.

[ERI 95] Eriksson, K., Estep, D., Hansbo, P., Johnson, C., "Introduction to Numerical Methods for Differential Equations", *Acta Numerica*, 1995, pp. 105–158.

[GIL 97] Giles, M., Larson, M., Levenstam, M., Süli, E., "Adaptive Error Control for Finite Element Approximations of the Lift and Drag Coefficients in Viscous Flow", Technical Report NA-97/06, Comlab, Oxford University, 1997.

[GOD 59] Godunov, S.K., "A Finite Difference Method for the Numerical Computation of Discontinuous Solutions of the Equations of Fluid Dynamics", *Mat. Sb.*, vol. 47, 1959.

[GIL 99] Giles, M., Pierce, N.A., "Improved Lift and Drag Estimates Using Adjoint Euler Equations", Technical Report 99-3293, AIAA, Reno, NV, 1999.

[HAR 83] Harten, A., "High Resolution Schemes for Hyperbolic Conservation Laws", *J. Comp. Phys.*, vol. 49, 1983, pp. 357–393.

[HAR 89] Harten, A., "ENO Schemes with Subcell Resolution", *J. Comp. Phys.*, vol. 83, 1989, pp. 148–184.

[HAR 87] Harten, A., Osher, S., Engquist, B., Chakravarthy, S., "Uniformly High-Order Accurate Essentially Nonoscillatory Schemes III", *J. Comp. Phys.*, vol. 71, n°2, 1987, pp. 231–303.

[JOH 86] Johnson, C., Pitkäranta, J., "An Analysis of the Discontinuous Galerkin Method for a Scalar Hyperbolic Equation", *Math. Comp.*, vol. 46, 1986, pp. 1–26.

[JOH 95] Johnson, C., Rannacher, R., Boman, M., "Numerics and Hydrodynamic Stability Theory: Towards Error Control in CFD", *SIAM J. Numer. Anal.*, vol. 32, 1995, pp. 1058–1079.

[KRO 96] Kröner, D., Rokyta, M., Wierse, M., "A Lax-Wendroff Type Theorem for Upwind Finite Volume Schemes in 2-D", *East-West J. Numer. Math.*, vol. 4, n°4, 1996, pp. 279–292.

[KRO 95] Kröner, D., Sebastian, S., Rokyta, M., "Convergence of Higher Order Upwind Finite Volume Schemes on Unstructured Grids for Scalar Conservation Laws in Several Space Dimensions", *Numer. Math.*, vol. 71, n°4, 1995, pp. 527–560.

[ODE 99] Oden, J.T., Prudhomme, S., "Goal-Oriented Error Estimation and Adaptivity for the Finite Element Method", Technical Report 99-015, TICAM, U. Texas, Austin,TX, 1999.

[PRU 99] Prudhomme, S., Oden, J.T., "On Goal-Oriented Error Estimation for Elliptic Problems: Application to the Control of Pointwise Errors", *Comp. Meth. Appl. Mech. and Eng.*, 1999, pp. 313–331.

[PER 97] Parashivoiu, M., Peraire, J., Patera, A., "A Posteriori Finite Element Bounds for Linear-Functional Outputs of Elliptic Partial Differential Equations", *Comput. Meth. Appl. Mech. Engrg.*, vol. 150, 1997, pp. 289–312.

[REE 73] Reed, W. H., Hill, T. R., "Triangular Mesh Methods for the Neutron Transport Equation", Technical Report LA-UR-73-479, Los Alamos National Laboratory, Los Alamos, New Mexico, 1973.

[Sul 98] Süli, E., "A Posteriori Error Analysis and Adaptivity for Finite Element Approximations of Hyperbolic Problems", in Kröner, Ohlberger, and Rohde, editors, *An Introduction to Recent Developments in Theory and Numerics for Conservation Laws*, volume 5 of *Lecture Notes in Computational Science and Engineering*, Springer-Verlag Pub., Heidelberg, 1998, pp. 122–194.

[SHU 88] Shu, C.-W., Osher, S., "Efficient Implementation of Essentially Non-Oscillatory Shock-Capturing Scheme", *J. Comp. Phys.*, vol. 77, 1988, pp. 439–471.

[VAN 93] Vankeirsbilck, P., *Algorithmic Developments for the Solution of Hyperbolic Conservation Laws on Adaptive Unstructured Grids*, PhD thesis, Katholiek Universiteit van Leuven, 1993.

[LEE 79] van Leer, B., "Towards the Ultimate Conservative Difference Schemes V. A Second Order Sequel to Godunov's Method", *J. Comp. Phys.*, vol. 32, 1979.

[ZIE 92] Zienkiewicz, O.C., Zhu, J.Z., "The Superconvergent Patch Recovery and A Posteriori Error Estimates. Part I: the Recovery Technique", *Int. J. Numer. Meth. Engrg.*, vol. 33, 1992, pp. 1331–1364.